Supporting Information For:

Fe L-edge XAS of Low Spin Heme Relative to Non-heme Fe Complexes: Delocalization of Fe d electrons into the Porphyrin Ligand

Rosalie K. Hocking,[1] Erik C. Wasinger,[1] YiLong Yan,[1]
Frank M. F. deGroot,[2] F. Ann Walker,[3] Keith O. Hodgson,[1,4]*
Britt Hedman,[4]* and Edward I. Solomon[1]*

[1]*Department of Chemistry, Stanford University, Stanford, California 94305.*
[2]*Department of Inorganic Chemistry and Catalysis, Utrecht University, Sorbonnelaan 16, 3584, The Netherlands.*
[3]*Department of Chemistry, The University of Arizona, Tucson, Arizona 85721*
[4]*Stanford Synchrotron Radiation Laboratory, SLAC, Stanford University, Stanford, California 94309.*

Complete reference 73

(73) Baerends E.J.; Berces A.; Bo C.; Boerrigter P.M.; Cavallo L.; Deng L.; Dickson R. M.; Ellis D. E.; Fan L.; Fischer T. H.; Fonseca Guerra C.; van Gisbergen S.J.A.; Groaeneveld J. A.; Gritsenko O. V.; Harris F. E.; van den Hoek P.; Jacobsen H.; van Kessel G.; Kootstra F.; van Lengthe E.; Osinga V. P.; Philipsen P. H. T.; Post D.; Pye C. C.; Ravenek W.; Ros P.; Schipper R. T.; Schreckenbach G.; Snijders J. G.; Sola M.; Swerhone D.; teVelde G.; Vernooijs P.; Versluis L.; Visser O.; van Wezenbeek E.; Wiesenekker G.; Wolff S. K.; Woo T. K.; Ziegler T. Amsterdam, 2000, 2000.01.

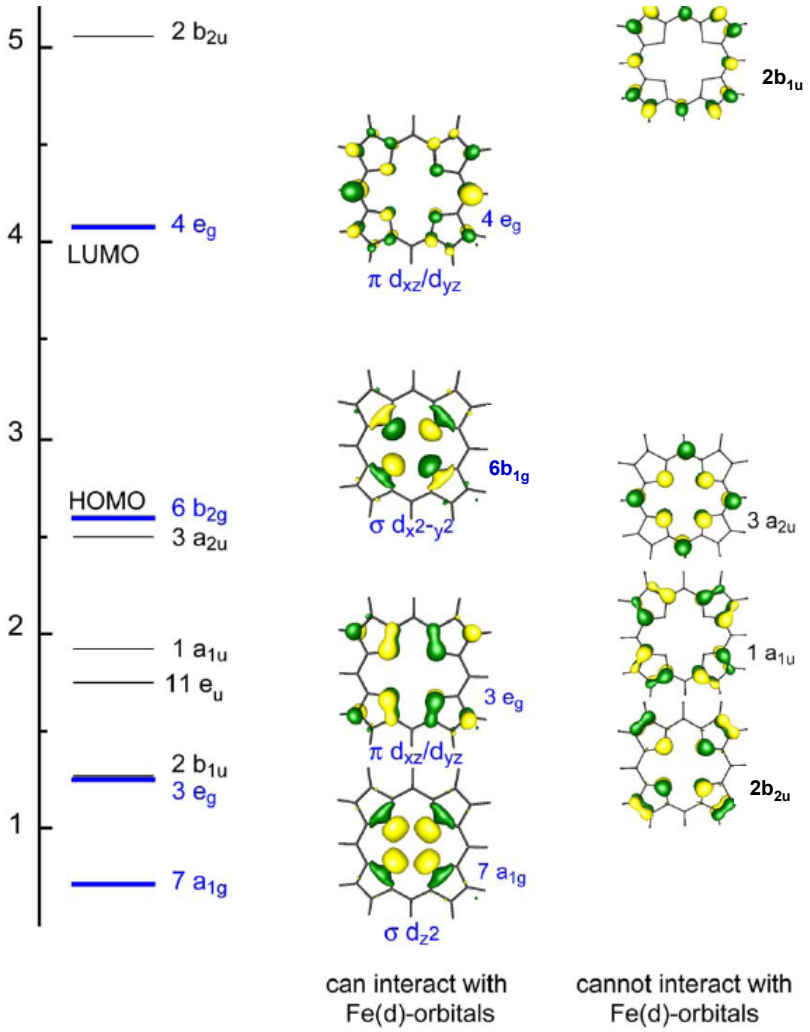

Figure S1. Heme Orbitals in D_{4h} symmetry adapted from the supporting information of Andrea Decker, Edwards I. Solomon "Comparison of FeIV=O heme and non-heme species: Electronic structures, bonding and reactivities. Angew Chem Int. Ed.. (2005 44(15) 2252

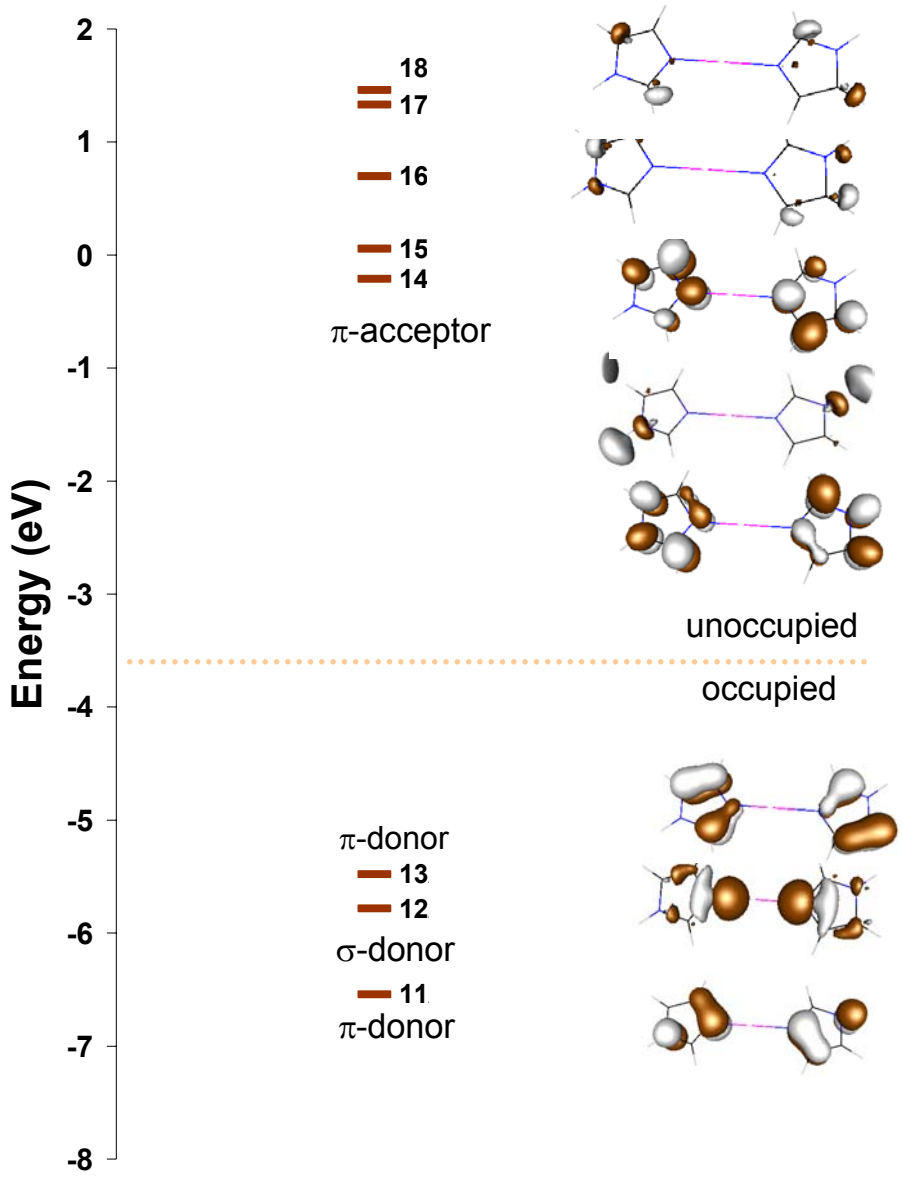

Figure S2. Orbitals of ImH capable of interacting with the d-manifold.

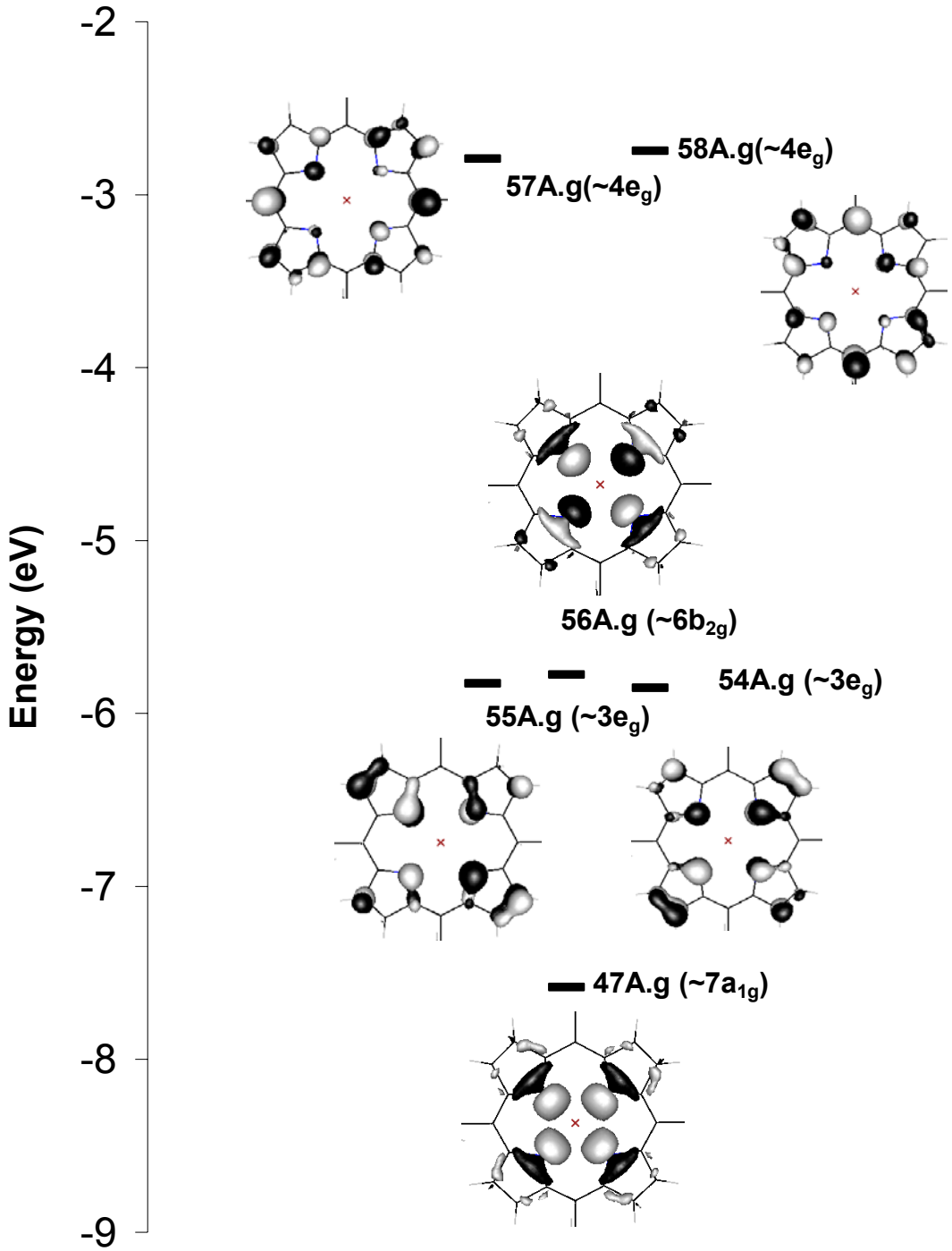

Figure S3. Heme orbitals calculated under C_i symmetry

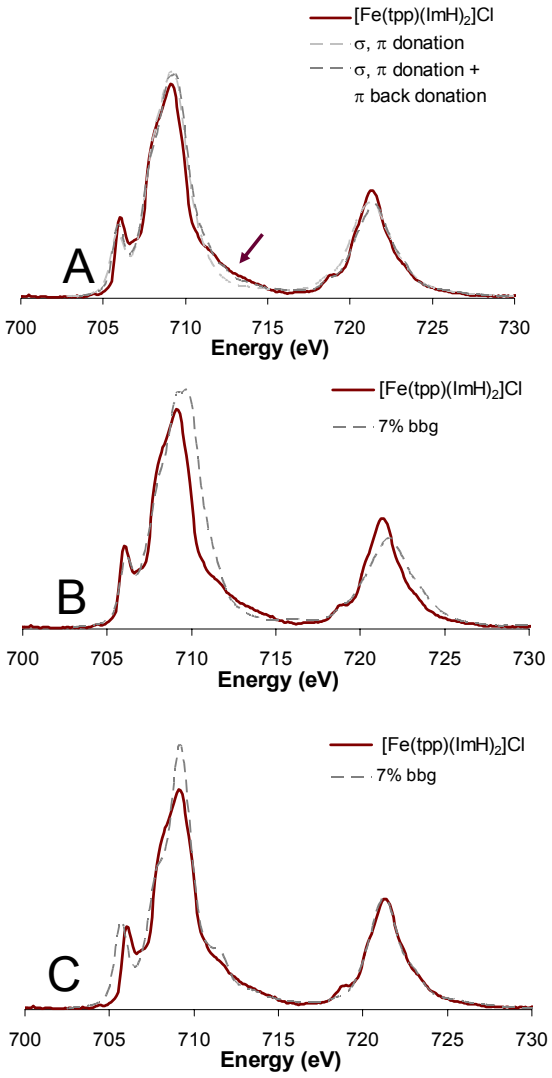

Figure S4. The effect of the addition of back-bonding to the simulation of $[Fe(tpp)(ImH)_2]Cl$. A. best fit which includes back-bonding is compared to the fit included in the paper. B and C are examples of simulations with around 7% back-bonding. The differences in the simulations arise from differences in the energy position of π*.

Table S1. Table of VBCI input parameters, and projected values in terms of total intensity for Figure 5. VBCI Input parameter and projected covalency of simulations, for all three simulations EG2=0.0, EF2=-2.0, 10Dq=2.8, Ds=0.04, Dt=0.04

	Input Parameters				**% Metal Character in Orbital**			
	B1	**A1**	**B2**	**E1**	**B1**	**A1**	**B2**	**E1**
Spectra A	3.4	3.4	0.9	0.9	48	48	76	76
Spectra B	4.0	4.0	1.0	3.0	51	56	N/A	56
Spectra C (best fit)	4.4	3.2	1.0	3.0	48	61	N/A	52

Table S2. Parameter values used in the two-configuration VBCI simulations for both heme and non-heme Fe.

	EG2	**EF2**	**Δ**	**10Dq**	**Dt**	**Ds**	**T(b^1)**	**T(a^1)**	**T(b^2)**	**T(e^1)**
$[Fe(tacn)_2]Cl_3^1$ d^5-d^6	2.8	0.8	3.56	2.2	0.00	0.00	3.4	3.4	0.9	0.9
$[Fe(tpp)(ImH)_2]Cl$ d^5-d^6	0.0	-2.0	0.49	2.8	0.04	0.04	4.4	3.2	1.0	3.0
$[Fe(tacn)_2]Cl_2^1$ d^6-d^7	2.8	2.1	3.45	1.8	0.00	0.00	1.8	1.8	0.3	0.3
$[Fe(tpp)(ImH)_2]$ d^6-d^5	0.9	1.2	0.2	2.3	0.02	0.03	0.0	0.0	0.3	0.77
$K_4[Fe(CN)_6]^2$ d^6-d^5	-2.0	-1.0	0.3	3.7	0.00	0.00	0.0/1.0	0.0/1.0	2.0	2.0

*These parameters are for the $2p^6$ initial state and $2p^5$ final sate. The ligand field parameters T and Δ will decrease upon going to the final state and the effects of changing their values in the $2p^5$ final state have been evaluated, see Figure S9. It is found that final state changes do not affect the results of the DOC analysis of the initial state in these highly covalent systems.

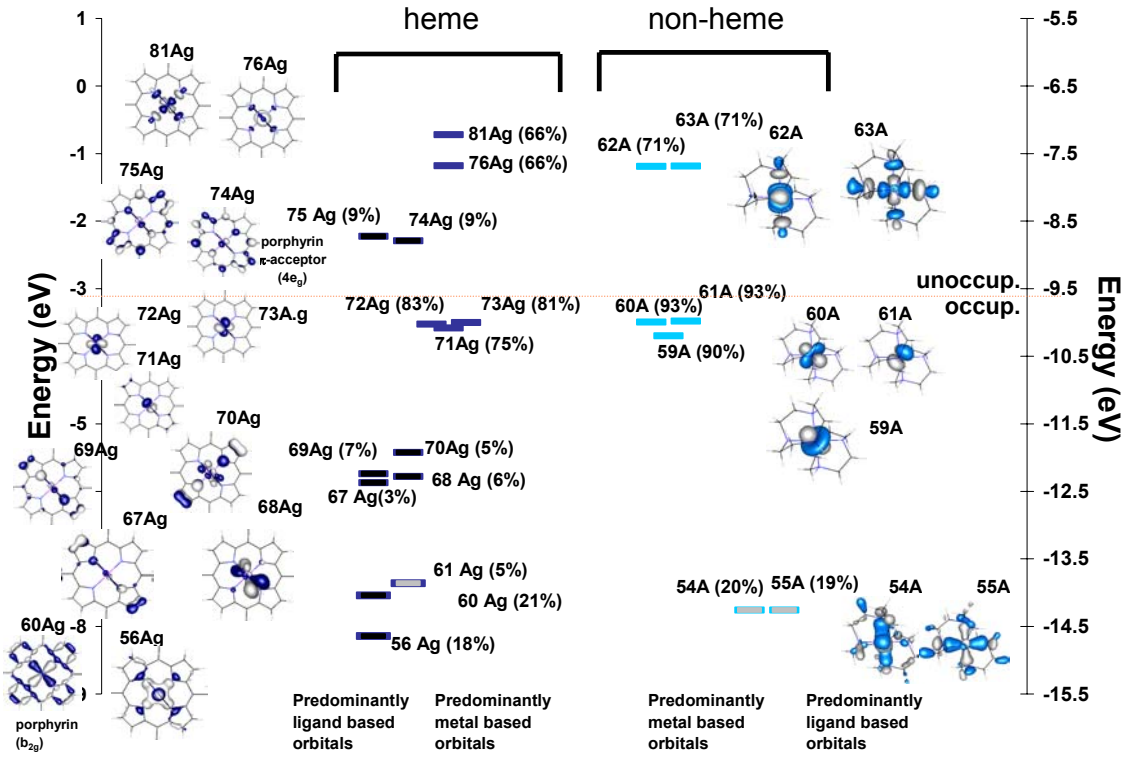

Figure S5. Comparison of energy levels in Fe(II) heme [Fe(tpp)(ImH)$_2$] and non-heme Fe [Fe(tacn)$_2$]$^{2+}$. Orbitals are numbered as the output from ADF, the % metal character in each orbital is given in brackets after orbital number. Orbitals predominantly metal in character are fully colored. Those which are predominantly porphyrin are colored black and those predominantly ImH (heme complex) or tacn(non-heme complex) are colored grey. The main contributors to each of the MO of the compound [Fe(tpp)(ImH)$_2$] are given in Table 2 and the Supporting Information following these figures

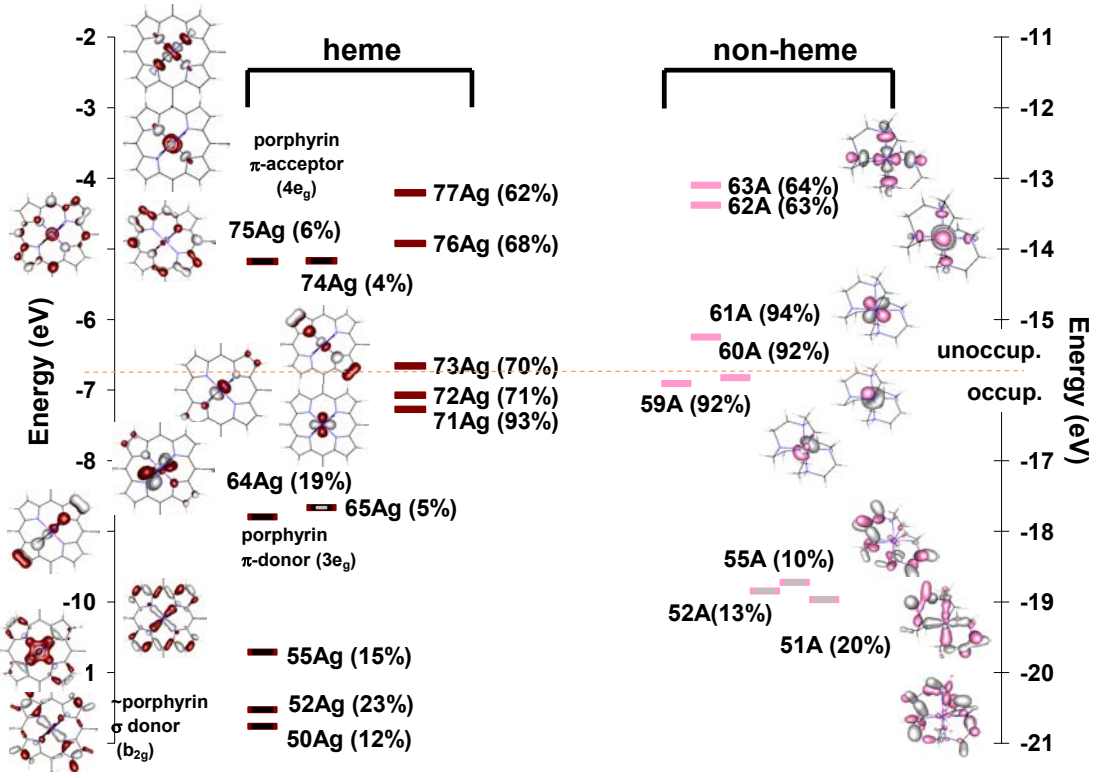

Figure S6. Comparison of energy levels in Fe(III) heme *vs* non heme $[Fe(tpp)(ImH)_2]^+$ orbitals are colored red and $[Fe(tacn)_2]^{3+}$ orbitals are colored in pink. Orbitals are numbered as the output from ADF and the % metal character in each is given in brackets after the number. Orbitals predominantly metal in character are fully colored. Those which are predominantly porphyrin (tpp) are colored black and those predominantly ImH(heme) or tacn(non-heme) are colored in grey. The main contributors to each of the MO of the compound $[Fe(tpp)(ImH)_2]$ are given in Table 2 and the Supporting Information following these figures

Orbital deconvolutions for Figures 2 and 3 (Note that key orbital contributions are given in Table 2 of the text.)

[Fe(tpp)(ImH)$_2$]

ImH (heme) or tacn(non-heme) are colored grey. The main contributors to each of the MO of the compound [Fe(tpp)(ImH)$_2$] are: **56 Ag.** 33%(tpp-49Ag) + 22%(tpp-42Ag) + 18%(Fe-d_{z2}) + 18%(ImH-12 Ag) +5%(tpp-other) **60 Ag.** 50%(tpp-b_{2g}) + 22%(Fe-d_{x2-y2}) + 12%(tpp-41Ag) + 14%(tpp-other)+ (ImH-3% other) **61 Ag.** 84% (ImH-11Ag) + 5%(Fe-d_{xz}) + 5%(tpp-35Ag) **67 Ag.** 51% (tpp-52Ag) + 24% (tpp-51Ag) + 11% (52 Ag) 8%(tpp-67Ag) + 4%Fe- d_{yz} **68 Ag.** 89%(ImH-13Ag) + 4% (ImH-11Ag) + 9.5%(54Ag) + 2% (Fe-d_{xz}) **69 Ag.** 56%(tpp-3e_g) + 22%(tpp-52Ag) + 7% (Fe-d_{yz}) + 11% (tpp-other) +7% (Fe-d_{xz}/d_{yz}/d_{xy}) **70 Ag.** 60%(tpp-3e_g) +11%(ImH-other) + 12%(tpp-other) + 5% (Fe-d_{xz}/d_{yz}/d_{xy}) **71Ag** 75%(Fe-d_{yz}) + 15%(tpp-3e_g) + 4% (tpp-4e_g) + 5% (tpp-other) **72Ag** 83%Fe(d_{xy}+d_{xz}) + 7% (tpp-4eg) + 4% (tpp-other) **73 Ag** 82% (Fe-d_{xy}+d_{xz}) + 5% (tpp-4e_g) + 5% (ImH-other)+ 5% (tpp-other) **74Ag** 90% (tpp-4e_g) + 9%(Fe-d_{xz}) **75Ag** 90% (tpp-4e_g) + 9% Fe(d_{yz}) **76Ag** 65% (Fe-d_{z2}) + 9% (49Ag-tpp) + 2%(tpp-other)+ 18%(ImH-12Ag) + 6% (ImH-other). **81Ag** 67% (Fe-d_{x2-y2}) + 27% (b_{2g}-tpp) + 4%(tpp-other)

[Fe(tpp)(ImH)$_2$]Cl

Betas. 50Ag 33%(tpp-4Ag) 16%(tpp-40Ag) + 16%(tpp-6b_{2g}) + 10%(Fe-d_{x2-y2}) + 2 %(Fe-dz^2); **52Ag** 38%(tpp-51Ag) + 23%(Fe-dz^2) + 15%(ImH-12Ag); **55Ag** 36%(tpp-41Ag) + 34 % (tpp-6b_{2g}) + 15% (Fe-d_{x2-y2}) + 7% (tpp-45 Ag); **64Ag** 71% (tpp-3e_g) + 19% (Fe-d_{yz}) **65Ag.** 59% (ImH-13Ag) +19% (tpp-3e_g) + 5%(Fe-d_{xz}); **71Ag** 93%Fe(d_{xy}); **72Ag** 71%(Fe-d_{yz}) + 23% (tpp-3e_g) + 1% (tpp-4e_g) **73Ag** 70%(Fe-d_{xz}) + 17%(tpp-3e_g) + 5%(tpp-4e_g) **74Ag** 95%(tpp-4e_g) + 4% d_{yz} **75Ag** 95%(tpp-4e_g) +6%(Fe-d_{xz}) **76 Ag** 59%(Fe-d_{z2}) + 20%(ImH-12Ag) + 5%(Fe-d_{x2-y2}) **77Ag** 61%(Fe-d_{x2-y2}) + 29%(tpp-6b_{2g}) + 6%(Fe-d_{z2}). **Alphas. 71Ag** 73%(tpp-3e_g) + 25% (Fe-d_{xz}); **72 Ag** 92%(Fe-d_{xy}) **73Ag** 61%(Fe-d_{xz}) + 35%(Fe-3e_g) **74 Ag** 49%(Fe-d_{z2}) + 2%(Fe-d_{x2-y2}) + 20%(ImH-12Ag) + 16% (tpp-4e_g) **75 Ag** 81%(tpp-4e_g) + 10%(Fe-d_{z2}) **76 Ag** 96%(tpp-4e_g) + 2%(Fe-d_{yz}) **77Ag** 61%(Fe-d_{x2-y2}) + 35%(tpp-6b_{2g}) + 2%(Fe-d_{z2}).[3]

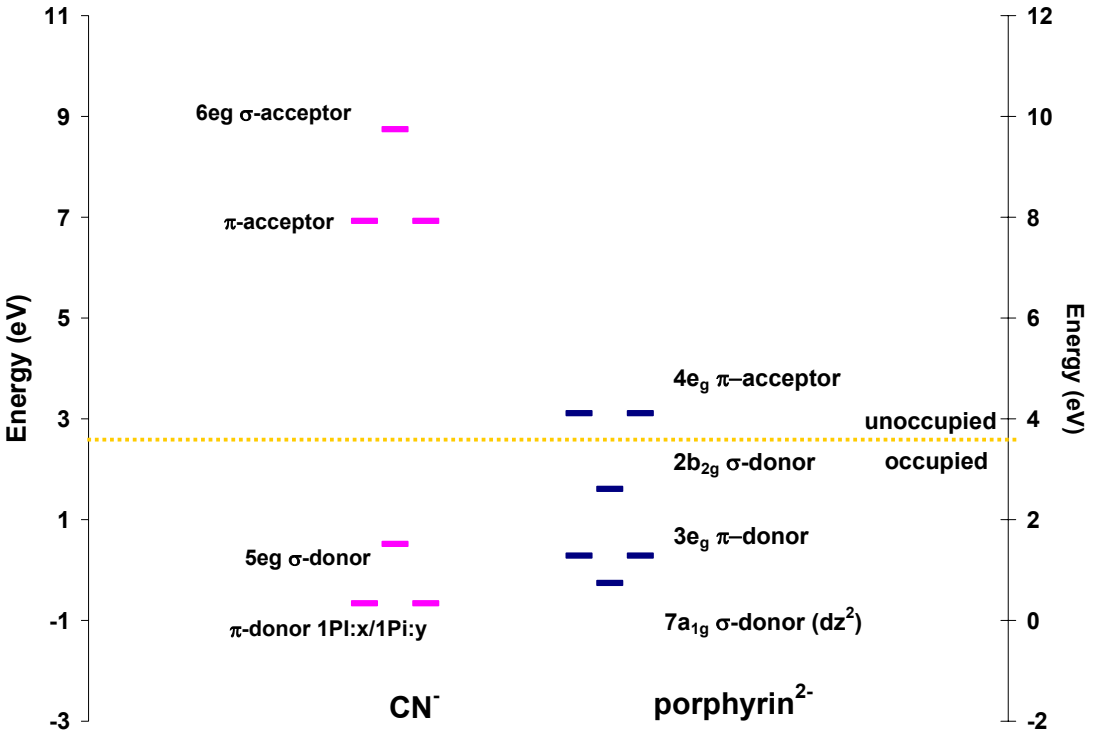

Figure S8. A comparison of the relative energy levels of the CN^- σ donor and the CN^- π acceptor.

Table S3. Hartree-Fock parameters (in eV) for Fe(II) $2p^6Fe3d^6 \rightarrow 2p^53d^7$ and for Fe(III) $2p^6Fe3d^5 \rightarrow 2p^53d^6$ transitions

	(3d,3d)			**(2p,3d)**			
	ζ_{3d}	F^{2**}	F^{4**}	ζ_{2p}	F^{2**}	G^{1**}	G^{3**}
Fe $3d^6$	0.052	8.772	5.452	-	-	-	-
Fe $3d^6$	0.046	7.809	4.814	-	-	-	-
Fe $2p^53d^7$	0.067	9.423	5.861	8.2	5.434	4.033	2.275
Fe $2p^53d^8$	0.059	8.498	5.28	8.2	4.914	3.573	2.030
Fe $3d^5$	0.059	9.634	6.028	-	-	-	-
Fe $3d^6$	0.052	8.772	5.452	-	-	-	-
Fe $2p^53d^6$	0.074	10.244	6.418	8.2	5.956	4.452	2.532
Fe $2p^53d^7$	0.067	9.423	5.861	8.2	5.434	4.003	2.275

**Note that these numbers are 80% of the Hartree-Fock calculated values (i.e κ=0.8) [4-6] They have been reduced to account for the known over-estimation of electron-repulsion by Hartree-Fock Theory.

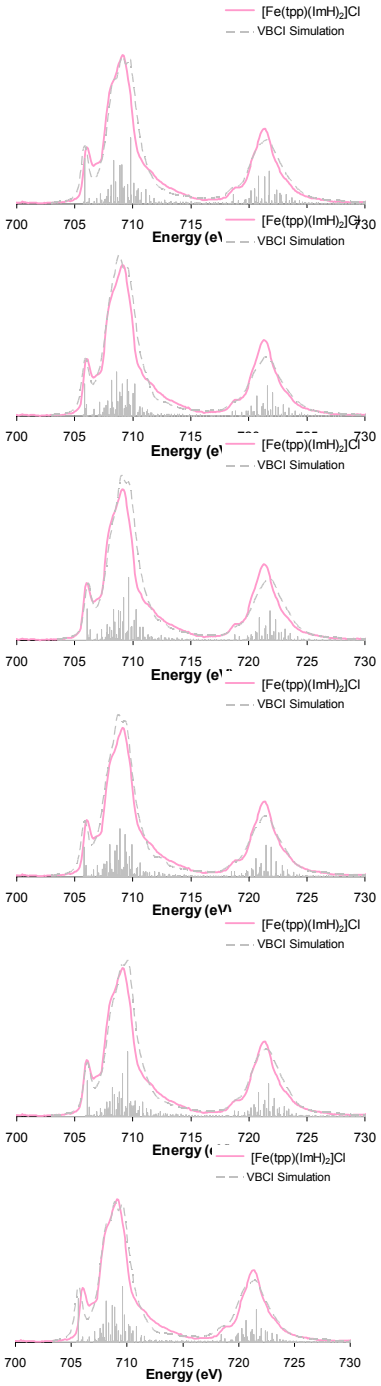

Figure S9. The effect of changing final state parameters on the simulations of [Fe(tpp)(ImH)$_2$]Cl. The spectra are not substantially changed and thus the mixing coefficients obtained for the projection method do not change from those reported in the text.

(1) Wasinger E. C.; deGroot F. M. F.; Hedman B.; Hodgson K. O.; Solomon E. I. *J. Am. Chem. Soc.* **2003**, *125*, 12894-12906.

(2) Hocking R. K.; Wasinger E. C.; deGroot F. M. F.; Hodgson K. O.; Hedman B.; Solomon E. I. *J. Am. Chem. Soc.* **2006**, *128*, 10442-10451.

(3) Scarrow R. C.; Riley P. E.; Kamal Abu-Dari.; White David L. *Inorg. Chem.* **1985**, *24*, 954-967.

(4) Arrio M.-A.; Sianctavit Ph.; Cartier dit Moulin Ch.; Mallah T.; Verdaguer M.; Pellegrin E.; Chen C. T. *J. Am. Chem. Soc.* **1996**, *118*, 6422-6427.

(5) Arrio M.-A.; Scuiller A.; Sainctavit Ph.; Cartier dit Moulin Ch.; Mallah T.; Verdaguer M. *J. Am. Chem. Soc.* **1999**, *121*, 6414-6420.

(6) Cartier dit Moulin Ch.; Villain F.; Bleuzen A.; Arrio M. A.; Sainctavit C.; Lomenech C.; Escax V.; Baudelet F.; Dartyge E.; Gallet J. J.; Verdaguer M. *J. Am. Chem. Soc.* **2000**, *122*, 6653-6658.